Soft Matter

PAPER

View Article Online
View Journal

Cite this: DOI: 10.1039/c4sm02896a

Enzyme-responsive protein/polysaccharide supramolecular nanoparticles†

Xiao-Fang Hou, Yong Chen and Yu Liu*

Received 30th December 2014
Accepted 4th February 2015

DOI: 10.1039/c4sm02896a

www.rsc.org/softmatter

Biocompatible and enzyme-responsive supramolecular assemblies have attracted more and more interest in biomaterial fields, and find many feasible applications especially in the controlled drug release at specific sites where the target enzyme is located. In this work, novel supramolecular nanoparticles were successfully constructed from two biocompatible materials, *i.e.* a cyclic polysaccharide named sulfato-β-cyclodextrin (SCD) and a protein named protamine, through non-covalent association, and fully characterized by means of atomic force microscopy (AFM) and high-resolution transmission electron microscopy (TEM). Significantly, the disassembly of the resulting nanoparticles can respond especially to trypsin over other enzymes. Owing to their trypsin-triggered disassembly behaviors, these nanoparticles can efficiently release the encapsulated model substrate in a controlled manner. That is, the model substrate can be encapsulated inside the nanoparticles with a high stability and released when treated with trypsin.

Introduction

Stimuli-responsive assemblies have become an extraordinarily fascinating topic in recent years due to their prospective use in the fields of chemistry, biology, and materials science.[1] The stimuli that make the assemblies practically operational include pH, temperature, light, magnetic fields, redox, ionic strength, enzymes and so on.[2] Among them, the enzyme-responsive approach has attracted more and more interest in the construction of functional biomaterials, especially the targeted drug delivery system, for the following reasons: (1) enzymes play essential roles in most biochemical processes, and the enzyme-based approach exhibits excellent biocompatibility; (2) the targeted delivery of therapeutics to the enzyme-overexpressed sites through enzyme-based recognition is highly selective and efficient.[3] On the other hand, compared with traditional amphiphiles, supra-amphiphiles, which are constructed through non-covalent interactions or dynamic covalent bonds, are easy to prepare and tunably responsive to various external stimuli.[4] Therefore, one can believe that the combination of a supra-amphiphile strategy and an enzyme-responsive approach will provide new access to the design of smart and efficient carriers for biologically important matter. Recently, water-soluble macrocyclic compounds, such as cyclodextrins, sulfonatocalixarenes, pillars, and cucurbiturils, have been widely employed in building bioactive supramolecular assemblies including supra-amphiphiles.[5] Liu *et al.* constructed a series of supramolecular vesicles and micelles based on the complexation of *p*-sulfonatocalix[4]arene with cationic guest molecules as a delivery system of Alzheimer's disease drug or antipsychotic drug chlorpromazine.[6] Zhang *et al.* reported a series of cucurbituril-based water-soluble supramolecular polymers constructed *via* noncovalent interactions.[7] Scherman, Nau and co-workers developed several cucurbituril-based molecular containers and drug carriers *via* host–guest complexation and their applications in biomedical fields.[8] Wang *et al.* reported a multistimuli-responsive supramolecular vesicle based on water-soluble pillar[6]arene and its controlled drug release.[9] Li *et al.* reported a periodic three-dimensional supramolecular organic framework through the co-assembly of a tetratopic molecular block and cucurbit[8]uril as a supramolecular 'ion sponge' to absorb different kinds of anionic guests including drugs.[10]

More recently, we constructed a serine protease trypsin-responsive supramolecular vesicle from sulfonatocalixarenes and natural cationic protein protamine and investigated its serine protease trypsin-responsive controllable-release properties.[11] In this system, trypsin can convert protamine to amino acids and peptides with unparalleled specificity upon progressive cleavage of peptide bonds in the protein, leading to the disruption of the vesicle and the release of the drug at sites where trypsin is overexpressed. Following this idea, we construct herein a new trypsin-responsive protein/polysaccharide supramolecular assembly (protamine/SCD) from sulfato-β-cyclodextrin (SCD) and protamine (Scheme 1). The inherent advantages of using SCD and protamine as building blocks are (1) as compared with sulfonatocalixarenes, cyclodextrins (CDs), a series of cyclic polysaccharides mainly containing 6–8 glucose units linked by α-1,4 glucosidic bonds, are

Department of Chemistry, State Key Laboratory of Elemento-Organic Chemistry, Collaborative Innovation Center of Chemical Science and Engineering (Tianjin), Nankai University, Tianjin 300071, P. R. China. E-mail: yuliu@nankai.edu.cn

† Electronic supplementary information (ESI) available: Control experiments and supporting figures. See DOI: 10.1039/c4sm02896a

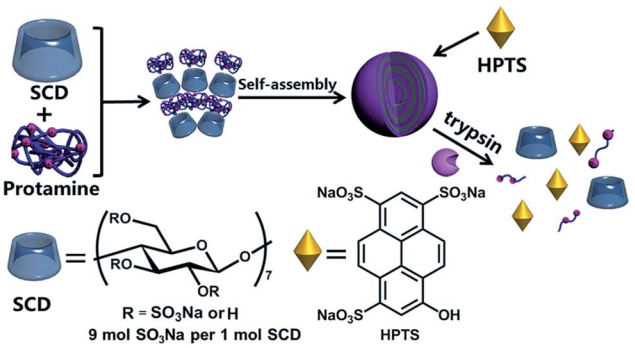

Scheme 1 Schematic illustration of protamine/SCD supramolecular nanoparticles.

water-soluble, nontoxic, and commercially available at low cost,[12] and more importantly, can include various inorganic/organic/biological molecules and ions in their hydrophobic cavity with high size/shape selectivity both in aqueous solution and in the solid state to construct nanostructured functional and bioactive materials;[13] (2) the negative charge density of SCD is much higher than that of sulfonatocalix[4]arene, which will lead to higher induced aggregation efficiency to cationic protamine; (3) protamine is a biocompatible natural protein with promising biological functions including binding DNA and providing a highly compact configuration of chromatin in the nucleus of the sperm and can be used as an excipient in insulin formulations;[14] (4) the polycationic structure of protamine can induce the supramolecular assembly of polyanionic SCD; (5) the enzyme trypsin can cleave protamine to amino acids and peptides with unparalleled specificity, leading to the enzyme-responsive disassembly of protamine/SCD nanoparticles. It is our special interest to develop a feasible strategy for producing new biocompatible supramolecular assemblies employing biocompatible materials, such as proteins and polysaccharides, as building blocks and biocompatible external stimuli, such as enzyme reactions, as the controlling method.

Results and discussion

Construction of supramolecular nanoparticles

As a natural cationic protein where nearly 67% of amino acid residues are positively charged, protamine is unable to form an amphiphilic self-assembly independently due to its high hydrophilicity. Excitingly, a simple mixture of SCD with protamine in aqueous solution shows the obvious Tyndall effect, indicating the formation of large aggregates in solution (Fig. S1†). In the control experiment, none of the free SCD, free protamine, or a mixture of SCD with arginine, the main composition of protamine, exhibited Tyndall effects under the same conditions.

The critical aggregation concentration (CAC) of SCD in the presence of protamine was measured by monitoring the dependence of the optical transmittance changes with increasing SCD concentration (Fig. 1). As seen from Fig. 1, the optical transmittance at 450 nm gradually decreased with the

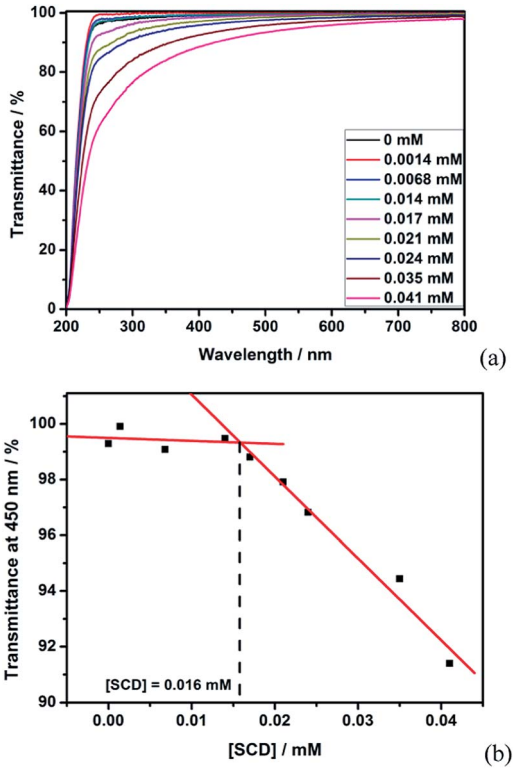

Fig. 1 (a) Optical transmittance of aqueous solutions containing protamine (50 μg mL^{-1}) and SCD at different concentrations at 25 °C. (b) Dependence of optical transmittance at 450 nm *versus* the concentration of SCD.

addition of SCD, indicating the formation of aggregates in solution. In addition, an inflection point at 0.016 mM was observed on the plot of optical transmittance at 450 nm *versus* the concentration of SCD, referring to a complexation-induced CAC value of SCD as 0.016 mM in the presence of protamine. In the control experiments, the optical transmittance at 450 nm showed no appreciable changes by using arginine instead of protamine, while SCD showed no tendency of self-aggregation, under the same conditions (see ESI Fig. S3†).

Moreover, the preferable mixing ratio between SCD and protamine was also determined. By gradually adding protamine to a SCD solution at a fixed concentration of 0.027 mM, the optical transmittance of protamine/SCD solution at 450 nm decreased rapidly and then gradually increased thereafter to a quasi-plateau, and the minimum was reached at a concentration of protamine as 20 μg mL^{-1}. The rapid decrease of optical transmittance indicated that a large aggregate was formed between protamine and SCD. Then, the addition of an excess amount of protamine led to the formation of a simple inclusion complex accompanied by the disassembly of the aggregate, resulting in the decrease of turbidity. This result means that the preferable mixing ratio for the formation of the protamine/SCD aggregate is 20 μg mL^{-1} protamine/0.027 mM SCD. Control experiments also show that, when replacing protamine by arginine, the resultant arginine/SCD solution presented no optical transmittance changes on increasing the arginine

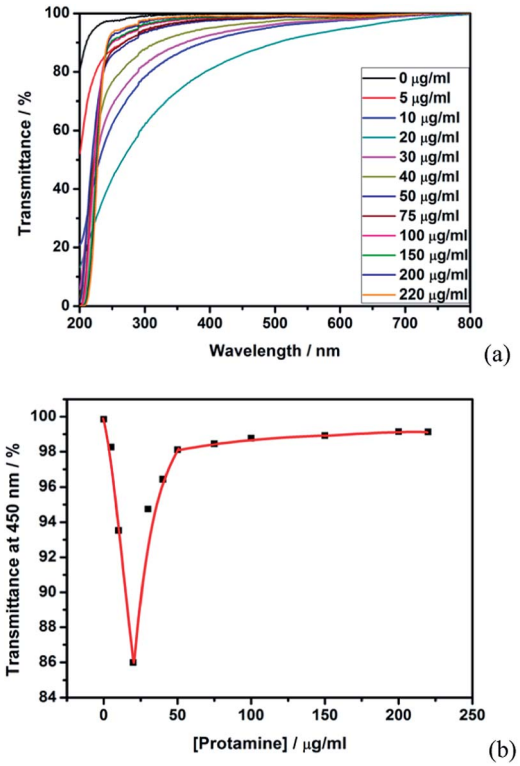

Fig. 2 (a) Optical transmittance of aqueous solutions of protamine at different concentrations in the presence of SCD (0.027 mM) at 25 °C. (b) Dependence of optical transmittance at 450 nm on the protamine concentration in the presence of SCD (0.027 mM).

concentration, indicating that the polycationic structure of protamine is an important factor leading to the protamine/SCD assembly (Fig. 2).

Dynamic light scattering (DLS), zeta potential, atomic force microscopy (AFM), and transmission electron microscopy (TEM) gave the structural and morphological information of the protamine/SCD assembly. The DLS results illustrated the existence of large aggregates of protamine/SCD with an average diameter of *ca.* 190 nm, accompanied by a narrow size distribution (Fig. 3a). It is well documented that the β-CD cavity could strongly bind the adamantyl group.[15] Therefore, the addition of an excess amount of 1-adamantanol to a solution of SCD could lead to the formation of the SCD/1-adamantanol inclusion complex *in situ*. When using this SCD/1-adamantanol inclusion complex instead of SCD in constructing the nanoparticles, the resultant protamine/SCD/1-adamantanol nanoparticles had a similar size (diameter 200 measured by DLS, Fig. S2†) to that of protamine/SCD nanoparticles (diameter 190 measured by DLS). Other control experiments showed that none of the free SCD, free protamine, a mixture of SCD with arginine, or a mixture of the SCD/1-adamantanol inclusion complex with arginine could form the nanoparticles. These jointly demonstrated that the electrostatic interactions between the polyanionic SCD and the polycationic protamine played an important role in the formation of nanoparticles.

The TEM image (Fig. 3b) shows a number of spherical particles with a diameter of 100–160 nm. The AFM image (Fig. 3c) also showed many spherical particles with a diameter of 100–200 nm and an average height of *ca.* 11.6 nm. Since SCD exists as a mixture of CDs randomly substituted by sulfonate groups with an average degree of substitution of 9, the resultant protamine/SCD nanoparticles are inhomogeneous to some extent. In addition, a comparison on the size of the protamine/SCD assembly with that of the protamine/*p*-sulfonatocalixarene assembly showed that, when the same amount of protamine was used, the resultant protamine/SCD assembly (diameter 100–160 nm by TEM, 190 nm by DLS) was more compact than the protamine/*p*-sulfonatocalixarene assembly (diameter 250 nm by TEM, 395 nm by DLS).[11] This indicated that SCD with higher negative charge density gave higher induced aggregation efficiency to cationic protamine than *p*-sulfonatocalixarene. Zeta potential measurements gave an average zeta potential of the protamine/SCD assembly as +4.94 mV, indicating that the nanoparticles still have the capability of associating anionic substrates (see ESI Fig. S4†).

Enzyme-responsive disassembly of the protamine/SCD assembly

The disassembly of the protamine/SCD assembly induced by trypsin was monitored by optical transmittance and TEM. When

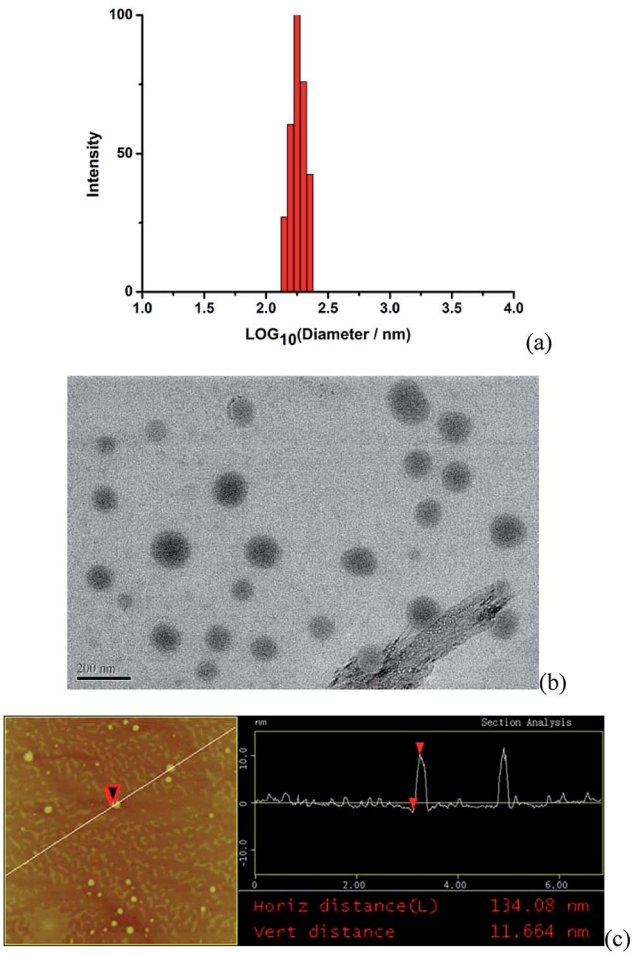

Fig. 3 (a) DLS data, (b) TEM image, and (c) AFM image of the protamine/SCD assembly ([SCD] = 0.027 mM, [protamine] = 20 μg mL^{-1}).

adding trypsin to a solution of the protamine/SCD assembly, the relatively low optical transmittance (82%) of the protamine/SCD assembly at 450 nm increases to 94% after 5 h (Fig. 4a), indicating the disappearance of the large aggregate. In addition, no spherical aggregates can be observed in TEM images after treating the protamine/SCD assembly with trypsin (Fig. 4b). Owing to the protection of the enveloping SCDs, the disassembly rate of the protamine/SCD assembly with trypsin is much slower than the hydrolysis rate of free protamine. Without trypsin, the protamine/SCD assembly is found to be very stable at room temperature, giving no appreciable changes of optical transmittance, turbidity or Tyndall effect even after 6 h (see ESI Fig. S5†).

To further investigate the crucial role of trypsin in the enzyme-triggered disassembly of protamine/SCD, the same amount of denatured trypsin (treated in boiling water for 1 h) was added to the protamine/SCD solution under the same conditions, giving no appreciable changes of optical transmittance, turbidity or Tyndall effect (see ESI Fig. S6†). This phenomenon clearly indicates that the disassembly of the protamine/SCD assembly mainly results from the cleavage of peptide bonds in the protein by trypsin, but not the introduction of a competitive polycation. In addition, some other enzymes including glucose oxide (GOX) and butyrylcholinesterase (BChE) are employed to investigate the specificity of trypsin in the disassembly. As shown in Fig. S7,† with the addition of GOX or BChE, the protamine/SCD solution showed no appreciable changes of optical transmittance (at 450 nm), turbidity or Tyndall effect density, demonstrating that this enzyme-responsive assembly exhibits a high specificity towards trypsin.

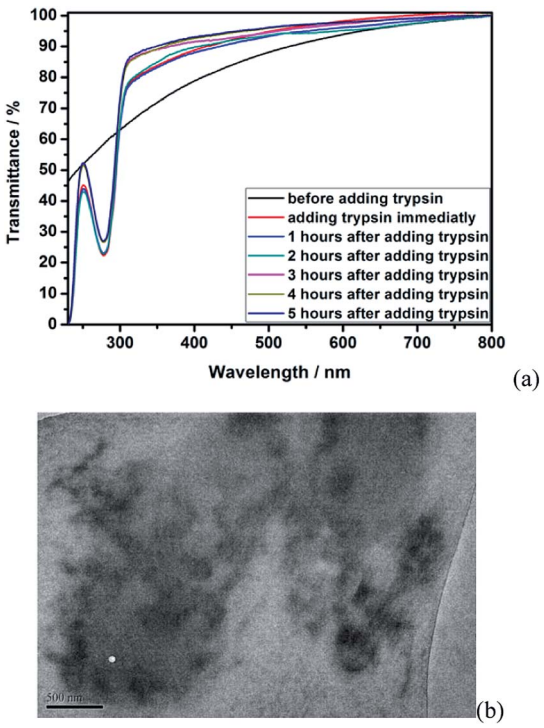

Fig. 4 (a) Optical transmittance of the protamine/SCD assembly before and after the addition of trypsin in water. (b) TEM image of the protamine/SCD assembly after the addition of trypsin. [SCD] = 0.027 mM, [protamine] = 20 μg mL^{-1}, and [trypsin] = 0.2 mg mL^{-1}.

Substrate loading and trypsin-triggered release

It is reasonable to expect that the trypsin-responsive disassembly can trigger a concomitant release of substrates sequestered within the interior of nanoparticles. In the substrate loading experiments, the trisodium salt of 8-hydroxypyrene-1,3,6-trisulfonic acid (HPTS) was selected as a model molecule, because the negatively charged HPTS was reported to be unable to form any assembly with protamine.[12] After loading free HPTS to the protamine/SCD assembly, the fluorescence intensity of HPTS quenched by 63% (Fig. S9†), indicating that the location of HPTS is in the interior of the protamine/SCD assembly. Moreover, after the anionic dye HPTS was loaded, the zeta potential of the nanoparticles decreased to +1.23 mV (Fig. S8†). In addition, fluorescence titration and NMR studies showed that the cavity of SCD barely included HPTS. Therefore, we deduced that HPTS should be encapsulated by the nanoparticles mainly through the electrostatic interactions between the positively charged nanoparticles and the anionic substrates. The release behaviors of HPTS with and without the addition of trypsin were investigated by means of fluorescence emission spectroscopy. As shown in Fig. S7† and 5, without trypsin, a very low release of entrapped HPTS was observed over a period of 5 h, indicating that the protamine/SCD assembly is highly stable toward leakage at room temperature in aqueous medium. However, the release rate was significantly enhanced when the protamine/SCD assembly was treated with trypsin, and more than 80% HPTS was released in 5 h, owing to the trypsin-triggered disassembly. In addition, nearly no HPTS release could be observed when treating the protamine/SCD assembly with other enzymes such as GOX or BChE. These phenomena imply that the present system is conceptually applicable as a controllable release model. That is, the assembly can encapsulate substrates,

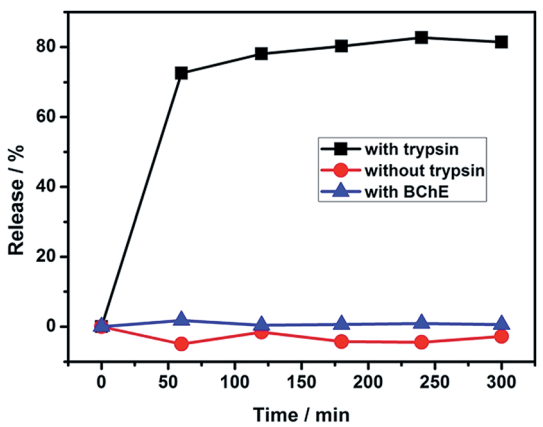

Fig. 5 Release of HPTS entrapped in the protamine/SCD assembly with and without trypsin, as well as with BChE. [SCD] = 0.027 mM, [protamine] = 20 μg mL^{-1}, [trypsin] = 0.2 mg mL^{-1}, [HPTS] = 0.01 mM, and [BChE] = 0.5 U mL^{-1}.

such as drugs, inside and release them at the sites where trypsin is over expressed.

Interestingly, when aniline was selected as a model substrate, the fluorescence intensity of aniline obviously decreased with the addition of protamine/SCD nanoparticles, which is consistent with the fluorescence behavior of aniline in the presence of SCD (Fig. S10†). The control experiment showed that either the change of ionic strength or the addition of a simple sulfonate anion could not decrease the fluorescence intensity of aniline under the same conditions. Therefore, the decreased fluorescence of aniline with the addition of protamine/SCD nanoparticles may be attributed to the inclusion of aniline by the SCD cavities in the nanoparticles, which consequently demonstrated the capability of SCD cavities in the nanoparticles for including model substrates. On this basis, further studies on the drug delivery system cooperatively utilizing SCD/drug inclusion complexation and assembly/substrate electrostatic interactions are in progress.

Conclusions

In conclusion, we successfully constructed supramolecular nanoparticles employing biocompatible protamine and polysaccharide as building blocks and the biocompatible enzyme-responsive approach as the controlling method. The resultant nanoparticles could be used as an enzyme-triggered controllable release model capable of site-specific response, which is reasonably expected to present the capability to increase the drug delivery efficiency and minimize the undesired side effects.

Experimental section

Materials

Protamine sulfate salt from salmon, trypsin from pancreas, BChE (from equine serum, 246 U mg^{-1}), and trisodium salt of 8-hydroxypyrene-1,3,6-trisulfonic acid (HPTS) were purchased from Sigma-Aldrich. Sulfatocyclodextrin (SCD) was purchased from Shandong Binzhou Zhiyuan Bio-Technology Co (the average degree of substitution is 9). Glucose oxidase (GOx) was purchased from Aladdin. Arginine was purchased from Bio Basic Inc. All of these were used without further purification. 1-Adamantanol and aniline were bought from the Guangfu chemical reagents company.

UV/Vis spectroscopy

UV/Vis spectra and the optical transmittance were recorded in a quartz cell (light path 10 mm) on a Shimadzu UV-3600 spectrophotometer equipped with a PTC-348WI temperature controller.

Fluorescence spectroscopy

Steady-state fluorescence spectra were recorded in a conventional quartz cell (light path 10 mm) on a Varian Cary Eclipse equipped with a Varian Cary single-cell Peltier accessory to control the temperature ($\lambda_{ex} = 339.0$ nm, bandwidth (ex) 2.5 nm, bandwidth (em) 5.0 nm).

TEM experiments

High-resolution TEM images were acquired using a Tecnai 20 high-resolution transmission electron microscope operating at an accelerating voltage of 200 keV. The sample for high-resolution TEM measurements was prepared by dropping the solution onto a copper grid, and the grid was then air-dried.

AFM experiments

The samples for AFM were analysed using a multi-mode IIIa AFM (Veeco Metrology, USA) in a tapping mode in air at room temperature. 2.7×10^{-5} M sample solutions were dropped onto newly clipped mica and then air-dried.

DLS measurements and zeta potential measurements

The sample solution for DLS measurements was prepared by filtering the solution through a 450 nm Millipore filter into a clean scintillation vial. The samples were examined on a laser light scattering spectrometer (BI-200SM) equipped with a digital correlator (TurboCorr) at 636 nm at a scattering angle of 90°. The zeta potential was measured using a ZetaPALS + BI-90 instrument (Brookhaven Co. USA).

HPTS-loaded nanoparticles

HPTS-loaded nanoparticles were prepared as follows: a certain amount of HPTS was added to a solution containing protamine and SCD, and then water was added until the volume of the solution reached 5 mL. The ultimate concentrations of HPTS, protamine, and SCD for HPTS-loaded nanoparticles in fluorescence spectroscopy and controlled-release experiments were 0.01 mM, 20 μg mL^{-1}, and 0.027 mM, respectively. One hour later, the prepared HPTS-loaded nanoparticles were purified by dialysis (molecular weight cut-off = 3500) in distilled water several times until the water outside the dialysis tube exhibited negligible HPTS fluorescence.

Acknowledgements

We thank the 973 Program (2011CB932502) and NSFC (91227107, 21432004, and 21272125) for financial support.

Notes and references

1 (*a*) X. Zhang, S. Rehm, M. M. Safont-Sempere and F. Würthner, *Nat. Chem.*, 2009, **1**, 623–629; (*b*) P. F. Kiser, G. Wilson and D. Needham, *Nature*, 1998, **394**, 459–462; (*c*) J. C. M. van Hest, *Nature*, 2009, **461**, 45–47; (*d*) D. M. Vriezema, M. C. Aragonès, J. A. A. W. Elemans, J. J. L. M. Cornelissen, A. E. Rowan and R. J. M. Nolte, *Chem. Rev.*, 2005, **105**, 1445–1489.

2 (*a*) D. Schmaljohann, *Adv. Drug Delivery Rev.*, 2006, **58**, 1655–1670; (*b*) J. Du, Y. Tang, A. L. Lewis and S. P. Armes, *J. Am. Chem. Soc.*, 2005, **127**, 17982–17983; (*c*) A. Almutairi,

S. J. Guillaudeu, M. Y. Berezin, S. Achilefu and J. M. J. Fréchet, *J. Am. Chem. Soc.*, 2008, **130**, 444–445; (*d*) J. R. Kumpfer and S. J. Rowan, *J. Am. Chem. Soc.*, 2011, **133**, 12866–12874; (*e*) L. M. Randolph, M.-P. Chien and N. C. Gianneschi, *Chem. Sci.*, 2012, **3**, 1363–1380.

3 (*a*) J.-M. Hu, G.-Q. Zhang and S.-Y. Liu, *Chem. Soc. Rev.*, 2012, **41**, 5933–5949; (*b*) N. Kamaly, Z. Xiao, P. M. Valencia, A. F. Radovic-Moreno and O. C. Farokhzad, *Chem. Soc. Rev.*, 2012, **41**, 2971–3010.

4 (*a*) X. Zhang and C. Wang, *Chem. Soc. Rev.*, 2011, **40**, 94–101; (*b*) Y. Wang, H. Xu and X. Zhang, *Adv. Mater.*, 2009, **21**, 2849–2864; (*c*) C. Wang, Z. Wang and X. Zhang, *Acc. Chem. Res.*, 2012, **45**, 608–618.

5 (*a*) K. Kim, N. Selvapalam, Y. H. Ko, K. M. Park, D. Kim and J. Kim, *Chem. Soc. Rev.*, 2007, **36**, 267–279; (*b*) D.-S. Guo and Y. Liu, *Chem. Soc. Rev.*, 2012, **41**, 5907–5921; (*c*) A. Harada, Y. Takashima and H. Yamaguchi, *Chem. Soc. Rev.*, 2009, **38**, 875–882; (*d*) C. Zhou, X. Chen, Y. Yun, J. Wang and J. Huang, *Langmuir*, 2014, **30**, 3381–3386; (*e*) C. Zhou, X. Chen, Q. Zhao, Y. Yun, J. Wang and J. Huang, *Langmuir*, 2013, **23**, 13175–13182; (*f*) G. Yu, X. Zhou, Z. Zhang, C. Han, Z. Mao, C. Gao and F. Huang, *J. Am. Chem. Soc.*, 2012, **134**, 19489–19497; (*g*) L.-L. Tan, H.-W. Li, Y.-C. Tao, S. X.-A. Zhang, B. Wang and Y.-W. Yang, *Adv. Mater.*, 2014, **26**, 7027–7031; (*h*) Y.-W. Yang, Y.-L. Sun and N. Song, *Acc. Chem. Res.*, 2014, **47**, 1950–1960.

6 (*a*) D.-S. Guo, K. Wang, Y. Wang and Y. Liu, *J. Am. Chem. Soc.*, 2012, **134**, 10244–10250; (*b*) Z.-B. Qin, D.-S. Guo, X.-N. Gao and Y. Liu, *Soft Matter*, 2014, **10**, 2253–2263; (*c*) S. Peng, K. Wang, D.-S. Guo and Y. Liu, *Soft Matter*, 2015, **11**, 290–296.

7 (*a*) Y. Liu, K. Liu, Z. Wang and X. Zhang, *Chem.–Eur. J.*, 2011, **17**, 9930–9935; (*b*) X. Tan, L. Yang, Z. Huang, Y. Yu, Z. Wang and X. Zhang, *Polym. Chem.*, 2015, **6**, 681–685; (*c*) Z. Huang, L. Yang, Y. Liu, Z. Wang, O. A. Scherman and X. Zhang, *Angew. Chem.*, 2014, **53**, 5351–5355.

8 (*a*) E. A. Appel, X. Loh, S. Jones, F. Biedermann, C. Dreiss and O. A. Scherman, *J. Am. Chem. Soc.*, 2012, **134**, 11767–11773; (*b*) D. Jiao, F. Biedermann, F. Tian and O. A. Scherman, *J. Am. Chem. Soc.*, 2010, **132**, 15734–15743; (*c*) T. Lee, E. Kalenius, A. I. Lazar, K. I. Assaf, N. Kuhner, C. H. Grun, J. Janis, O. A. Scherman and W. M. Nau, *Nat. Chem.*, 2013, **5**, 376–382; (*d*) K. I. Assaf and W. M. Nau, *Chem. Soc. Rev.*, 2015, **44**, 394–418.

9 (*a*) Y. Cao, X. Hu, Y. Li, X. Zou, S. Xiong, C. Lin, Y. Shen and L. Wang, *J. Am. Chem. Soc.*, 2014, **136**, 10762–10769; (*b*) Q. Duan, Y. Cao, Y. Li, X. Hu, T. Xiao, C. Lin, Y. Pan and L. Wang, *J. Am. Chem. Soc.*, 2013, **135**, 10542–10549.

10 (*a*) J. Tian, T.-Y. Zhou, S.-C. Zhang, S. Aloni, M. V. Altoe, S.-H. Xie, H. Wang, D.-W. Zhang, X. Zhao, Y. Liu and Z.-T. Li, *Nat. Commun.*, 2014, **5**, 5574; (*b*) K.-D. Zhang, J. Tian, D. Hanifi, Y.-B. Zhang, A. C.-H. Sue, T.-Y. Zhou, L. Zhang, X. Zhao, Y. Liu and Z.-T. Li, *J. Am. Chem. Soc.*, 2013, **135**, 17913–17918.

11 K. Wang, D.-S. Guo, M.-Y. Zhao and Y. Liu, *Chem.–Eur. J.*, DOI: 10.1002/chem.201303963.

12 K. Uekama, F. Hirayama and T. Irie, *Chem. Rev.*, 1998, **98**, 2045–2076.

13 (*a*) Y. Chen and Y. Liu, *Chem. Soc. Rev.*, 2010, **39**, 495–505; (*b*) Y. Chen, Y.-M. Zhang and Y. Liu, *Chem. Commun.*, 2010, **46**, 5622–5633.

14 F. Reynolds, R. Weissleder and L. Josephson, *Bioconjugate Chem.*, 2005, **16**, 1240–1245.

15 M. V. Rekharsky and Y. Inoue, *Chem. Rev.*, 1998, **98**, 1875–1918.

